Cylindrocyclophanes with Proteasome Inhibitory Activity from the Cyanobacterium *Nostoc* sp

George E. Chlipala[†], **Megan Sturdy**[†], **Aleksej Krunic**[†], **Daniel D. Lantvit**[†], **Qi Shen**[†], **Kyle Porter**[‡], **Steven M. Swanson**[†], and **Jimmy Orjala**[*,†]

Department of Medicinal Chemistry and Pharmacognosy, University of Illinois at Chicago, 833 S. Wood St., Chicago, Illinois, 60612 and Center for Biostatistics, The Ohio State University, Columbus, Ohio, 43221

Abstract

Material collected from a parkway in the city of Chicago afforded the isolation of a *Nostoc* species (UIC 10022A). The extract of this strain displayed significant inhibition of the 20S proteasome as well as antiproliferative activity against HT29, MCF7, NCI-H460, and SF268 cancer cell lines. A standardized dereplication protocol allowed for the rapid identification of three known (**11-13**) and nine new (**1-9**) chlorinated cylindrocyclophanes from less than 100 mg of organic extract. Scale-up isolation of **1-9** and **11-13** from a larger extract was guided by LC-UV-MS data. In addition, KBr enrichment of the culture media afforded the isolation of a brominated cylindrocyclophane (**10**). Biological evaluation of **1-5**, **9**, and **10-13** revealed a large range of activity against the 20S proteasome and allowed the determination of preliminary structure-activity relationships (SAR) of the cylindrocyclophane pharmacophore.

Cyanobacteria are considered a promising source for new pharmaceutical lead compounds and a large number of chemically diverse metabolites have been obtained from cyanobacteria.[1-5] In particular, members of the genus *Nostoc* have been a valuable source of biologically active compounds. The most prominent example is the cryptophycins, which were first isolated from a lichen cyanobiont.[6] These potent tubulin inhibitors eventually led to the development of a semi-synthetic clinical candidate.[7-9] Other examples of compounds isolated from cyanobacteria of the genus *Nostoc* are the cytotoxic nostocyclopeptides,[10] the antimicrobial nostocyclyne A,[11] as well as protease inhibitors such as the insulapeptolides,[12] nostopeptins,[13, 14] and microviridins G and H.[15] In all of these cases, the source organism was of freshwater or terrestrial origin.

As part of our ongoing effort to find novel bioactive natural products from cultured freshwater and terrestrial cyanobacteria from the U.S. Great Lakes region,[16] we have evaluated cyanobacterial extracts for inhibition of the 20S proteasome. The 20S proteasome is the catalytic core of the proteasome complex and plays a pivotal role in the control of cell proliferation, apoptosis, and differentiation in a variety of normal and tumor cells.[17-19] Currently, there is one proteasome inhibitor, bortezomib (Velcade) approved by the U.S. Food and Drug Administration.[20] Bortezomib was first approved in May 2003 for the treatment of multiple myeloma, however it has been shown to be effective against other

[*]To whom correspondence should be addressed. Tel: 1-312-996-5583. Fax: 1-312-413-4034. orjala@uic.edu.
[†]Department of Medicinal Chemistry and Pharmacognosy
[‡]Center for Biostatistics

cancers, e.g. lymphoma, prostate, and lung cancers.[17] Preliminary studies of the extract of *Nostoc* sp. (UIC 10022A), collected in Chicago, Illinois, revealed significant proteasome inhibitory activity as well as inhibition of growth in four cancer cell lines (HT-29, NCI-H460, SF268, and MCF7). HPLC MS/NMR dereplication allowed for identification of a series of cylindrocyclophanes as the active principles. Scale-up isolation using LC-UV-MS data to guide the fractionation yielded 9 new chlorinated cylindrocyclophanes. Herein we describe the isolation, structure determination and an in depth evaluation of the proteasome inhibitory activity of these new natural products.

Results and Discussion

The initial organic extract (83.5 mg) from a 4 L culture of *Nostoc* sp. (UIC 10022A) displayed significant, inhibitory activity against the 20S proteasome as well as antiproliferative activity against four cancer cell lines. This extract was subjected to a dereplication scheme, which included a Diaion VLC step with a subsequent semi-preparative HPLC fractionation and chemical analysis via ESI-TOF-MS and ^{1}H NMR spectroscopy. These standardized steps revealed the presence of three previously reported compounds, cylindrocyclophanes A (**11**), C (**12**), and F (**13**)[21] and 10 new analogues, cylindrocyclophanes A_4-A_1 (**1-4**), C_4-C_1 (**5-8**), and F_4 (**9**). A second extract of strain UIC 10022A from a 20 L culture was subjected to Diaion and reversed-phase HPLC to yield **1-9** and **11**-**13** in larger quantities. The HRESIMS data acquired from the dereplication of the initial extract were used in combination with LC-UV-MS data acquired on the second extract to guide the isolation of **1-9** and **11-13**.
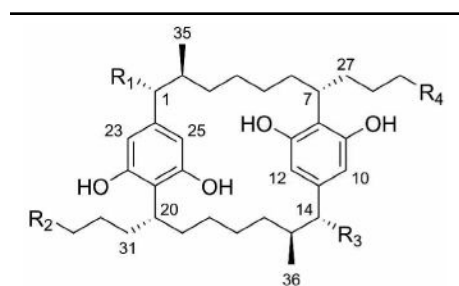
	R_1	R_2	R_3	R_4
1	OH	$CHCl_2$	OH	$CHCl_2$
2	OH	CH_2Cl	OH	$CHCl_2$
3	OH	CH_3	OH	$CHCl_2$
4	OH	CH_3	OH	CH_2Cl
5	OH	$CHCl_2$	H	$CHCl_2$
6	OH	CH_2Cl	H	$CHCl_2$
7	OH	CH_3	H	$CHCl_2$
8	OH	CH_3	H	CH_2Cl
9	H	$CHCl_2$	H	$CHCl_2$
10	OH	$CHBr_2$	OH	$CHBr_2$
11	OH	CH_3	OH	CH_3
12	OH	CH_3	H	CH_3
13	H	CH_3	H	CH_3

Cylindrocyclophane A_4 (**1**), the major metabolite, was obtained as a white, amorphous powder. The negative mode HRESI-TOF-MS data indicated a molecular formula of $C_{36}H_{52}Cl_4O_6$ ([M-H]⁻, *m/z* 719.2392) with an isotopic distribution pattern that was consistent with a tetrachlorinated molecule (70:100:53:13 M:M+2:M+4:M+6). The DEPTQ (Table 1) spectrum displayed only 18 carbon signals, indicating a symmetrical molecule. These results were consistent with a C_2 axis of symmetry, which was also found in the previously described cylindrocyclophane A (**11**).[21]

The ^{1}H NMR spectrum (Table 1) for **1** revealed a tetrasubstituted aromatic ring (δ_H 6.25 and 6.07), an oxygen-bearing benzylic methine (δ_H 3.74), a methyl doublet (δ_H 1.06), a methine triplet at δ_H 5.82, and 14 alkyl multiplets between δ_H 2.20 and 0.64. Analysis of the HSQC spectrum for **1** showed the downfield triplet (H-30/34, δ_H 5.82) was attached to a carbon (C-30/34) at δ_C 75.4. These chemical shifts were consistent with a dichlorinated methyl moiety.

Inspection of the ^{1}H NMR signals for the aromatic protons (H-10/23, δ_H 6.25 and H-12/25, δ_H 6.07) of **1** revealed a small coupling constant of 1.2 Hz. This *J* value was consistent with a meta relationship. The HMBC spectrum revealed correlations from these protons (H-10/23 and H-12/25) to the hydroxyl-bearing phenolic carbons (C-9/22, δ_C 159.0 and C-13/26, δ_C 157.1) as well as the quaternary aromatic carbon (C-8/21, δ_C 116.7) meta to these protons. The HMBC spectrum for **1** also revealed correlations between the benzylic proton signal (H-7/20, δ_H 3.19) and the aromatic carbons C-8/21, C-9/22, and C-13/26, confirming that the carbons C-9/22 and C-13/26 were attached to C-8/21 and C-8/21 in turn was attached to C-7/20. The HMBC spectrum for **1** revealed a correlation between the oxygen bearing benzylic proton signal (H-1/14, δ_H 3.74) and the aromatic carbons C-11/24 (δ_C 144.2), C-10/23 (δ_C 105.0), and C-12/25 (δ_C 108.8). These data confirmed that the aromatic carbons (C-10/23 and C-12/25) were attached to C-11/24 and that C-11/24 was attached to C-1/14.

Analysis of the COSY spectrum for **1** revealed that H-1/14 correlated with H-2/15 (δ_H 1.55). H-2/15, in turn, correlated with the methyl moiety (H₃-35/36, δ_H 1.06) as well as H-3b/16b (δ_H 0.64). The COSY data, in combination with HSQC data, also revealed correlations of H-3a/16a (δ_H 0.73) with H-4a/17a (δ_H 1.42), H-4b/17b (δ_H 0.83) with H-5b/18b (δ_H 0.72), H-5b/18b with H-6b/19b (δ_H 1.29), and H-6b/19b with H-7/10. The same process was used to assign the side chains (C-27/31 to C-30/34). Briefly, the COSY spectrum revealed the correlations from H-27b/31b (δ_H 1.48) to H₂-28/32 (δ_H 1.35), H₂-28/32 to H-29a/33a (δ_H 2.20), and H-29a/33a to H-30/34 (δ_H 5.82). Comparing these data with those previously reported by Moore et al.[21] and Bui et al.[22] we determined that **1** was 30,30,34,34-tetrachlorocylindrocyclophane A.

Cylindrocyclophanes A_3-A_1 (**2**-**4**) were also obtained as white, amorphous solids. The negative mode HRESI-TOF-MS data for **2**-**4** indicated molecular formulas of $C_{36}H_{53}Cl_3O_6$ ([M-H]⁻, *m/z* 685.2760), $C_{36}H_{54}Cl_2O_6$ ([M-H]⁻, *m/z* 651.3157) and $C_{36}H_{55}ClO_6$ ([M-H]⁻, *m/z* 617.3666), respectively. For each compound, the observed isotopic distribution patterns were consistent with the predicted degree of chlorination. The ^{1}H NMR spectra for **2**-**4** were similar to the spectrum of **1** indicating these compounds only differed by the degree of chlorination on C-30 and C-34. The ^{1}H NMR spectrum for **2** revealed a similar triplet at δ_H 5.82 with half the relative intensity as the signal observed in cylindrocyclophane A_4 and a new methylene triplet at δ_H 3.43 (H₂-34). The HSQC spectrum for **2** displayed a correlation of H₂-34 with δ_H 45.7 (C-34), which was consistent for 30,30,34-trichlorochlorocylindrocyclophane A. The ^{1}H NMR spectrum for **4** revealed a methylene triplet at δ_H 3.43 (H₂-30) and a methyl triplet at δ_H 0.79 (H₃-34), which indicated a 30-chlorocylindrocyclophane A. The ^{1}H NMR spectrum for **3** revealed a methine triplet at δ_H 5.82 (H-30) and a methyl triplet at δ_H 0.79 (H₃-34). These data indicated that the correct

structure of **3** was 30,30-dichlorocylindrocyclophane A. The ^{1}H, HSQC, and HMBC NMR data for **2-4** were compared with the data acquired for **1** as well as data published by Moore et al.[21] and Bui et al.[22] to assign the chemical shifts for **2-4**.

Cylindrocyclophanes C_4-C (**5-8**, **12**) were all obtained as white, amorphous solids. The negative mode HRESI-TOF-MS data for **5-8**, **12** indicated molecular formulas of $C_{36}H_{52}Cl_4O_5$ ([M-H]$^-$, m/z 703.2442), $C_{36}H_{53}Cl_3O_5$ ([M-H]$^-$, m/z 669.2824), $C_{36}H_{54}Cl_2O_5$ ([M-H]$^-$, m/z 635.3329), $C_{36}H_{55}ClO_5$ ([M-H]$^-$, m/z 601.3609) and $C_{36}H_{56}O_5$ ([M-H]$^-$, m/z 567.4019), respectively. Based upon the previously reported cylindrocyclophanes, it was proposed that **12** was cylindrocyclophane C as previously reported by Moore *et al.* and **5-8** were chlorinated analogs of **12**.[21]

The ^{1}H NMR spectra for **5-8** (Table 2) displayed similar signals as for **1-4** (Table 1), which indicated that these compounds followed the same chlorination pattern. However, a comparison of the molecular formulas revealed that the difference between these two series of compounds was that **5-8**, **12** contained only five oxygen atoms while **1-4** contained six oxygen atoms. The ^{1}H NMR spectrum for **7** revealed the same oxygen bearing benzylic proton (δ_H 3.75) as found in the ^{1}H NMR spectra for **1-4**, **11**. However, the ^{1}H NMR and HSQC spectra for **7** also revealed the presence of a benzylic methylene (δ_C 45.9, δ_H 2.61 and 1.83). From these data, it was deduced that C-1 was similar to C-1/14 found in **1-4**, **11**, however C-14 in **5-8**, **12** lacked the hydroxy moiety. The lack of symmetry of C-1 and C-14 complicated the structure elucidation of **5-8**, however the structures were solved using a combination of HMBC, COSY, and TOCSY data.

The ^{1}H NMR spectra for **5-8** displayed four different aromatic signals (δ_H ca. 6.24, 6.07, 6.02, and 5.98), as opposed to the two aromatic signals (δ_H 6.25, and 6.07) that were observed in the spectra of **1-4**, **11**. Correlations from the HMBC spectrum for **7** (Figure 1) revealed that protons H-23 (δ_H 6.24) and H-25 (δ_H 6.07) were part of the aromatic ring attached to C-1 (δ_C 81.8) and that protons H-10 (δ_H 6.02) and H-12 (δ_H 5.98) were part of the aromatic ring attached to C-14 (δ_C 45.9).

Further analysis of the HMBC spectrum for **7** revealed that the carbon at δ_C 117.8 ppm (C-21) was part of the aromatic ring containing H-23 (δ_H 6.24) and H-25 (δ_H 6.07). The HMBC spectrum for **7** also revealed a correlation between C-21 (δ_C 117.8) and H-31a (δ_H 1.93). Analysis of the TOCSY spectrum for **7** revealed that H-31a (δ_H 1.93) correlated to H_3-34 (δ_H 0.79), thus the side chain of C-31 to C-34 terminated in methyl moiety (Figure 1). Therefore, by a process of elimination, the side chain of C-27 to C-30 terminated in the dichloromethyl moiety.

The HMBC spectrum acquired for **8** revealed similar correlations between C-21 (δ_C 117.3) and H-23 (δ_H 6.07), H-25 (δ_H 6.24), and H-31b (δ_H 1.48). This, combined with the H31-H34 fragment determined by COSY, allowed for the proper assignment of the methyl at C-34, thus the chloromethyl moiety was assigned to position C-30. For compound **6**, the HMBC correlation between C-8 (δ_C 115.0) and H-27b (δ_H 1.52) was used in conjunction with the H27-H30 COSY fragment to properly assign the dichloromethyl moiety to position C-30. The structure elucidation of **5** was simplified by the fact that C-30 and C-34 were both dichloromethyl moieties, thus both side chains (C-27 to C-30 and C-31 to C-34) were, in essence, identical. The NMR data for **5-8** were compared with the data reported by Moore et al.[21] and Bui et al.[22] to properly assign all the spectroscopic data and to confirm the structures of cylindrocyclophane C_4 (**5**), cylindrocyclophane C_3 (**6**), cylindrocyclophane C_2 (**7**), and cylindrocyclophane C_1 (**8**).

Cylindrocyclophane F (**13**) was identified as a compound previously described by Moore et al. using ^{1}H NMR and MS data ([M-H]$^-$, m/z 551.4057).[21] Cylindrocyclophane F_4 (**9**) was

obtained as a white, amorphous solid. The negative mode HRESI-TOF-MS data for **9** indicated the molecular formula of $C_{36}H_{52}O_4Cl_4$ ([M-H]$^-$, *m/z* 687.2510), respectively. The ^{1}H NMR spectrum for **9** (Table 3) displayed signals similar to those for **1** and **5**; most notable was the presence of a methine triplet at δ_H 5.83 which correlated with δ_C 75.1 in the HSQC spectrum. As shown in **1** and **5**, these signals were consistent with a dichlorinated methyl moiety. The ^{1}H NMR spectrum for **9** lacked the signal of the oxygen attached benzylic methine found in **1** (H-1/14, δ_H 3.74) and **5** (H-1, δ_H 3.75). Instead, the ^{1}H NMR data for **9** revealed two signals (δ_H 2.58 and 1.83) and associated HSQC signal (δ_C 45.7) that were consistent with a benzylic methylene as found in **5** (14, δ_C 45.8, δ_H 2.61 and 1.82). The NMR spectra of **9** displayed only half of the expected NMR signals, revealing a similar C_2 axis of symmetry as found in **1**. This simplified the structure elucidation of **9**. The NMR data for **9** were compared with the data acquired for **1**-**8** to determine that **9** was 30,30,34,34-tetrachlorocylindrocyclophane F. Due to the low yield of **9** (approximately 0.1 mg), it was not possible to gain sufficient signal to noise in the HMBC spectrum to be able to assign the carbons (C-9/22 and C-13/26).

Configurational Analysis

The report by Moore et al. determined the absolute configuration of **11** using data acquired via Mosher's method and comparing the results with the X-ray crystallography data of nostocyclophane D.[21, 23] The same report also determined the absolute configurations of **12** and **13**, by a comparison of circular dichroism data. In the end, all three compounds were found to have the same absolute configuration at C-1, C-2, C-7, C-14, C-15, and C-20.[21] A similar relationship was found for **1**-**9**. The $^3J_{H-1/14,H-2/15}$ values for **1**-**4** ranged from 9.8-9.7 Hz. These values were similar to the value reported (10.3 Hz) by Moore et al. for **11**.[23] This large coupling constant (> 7 Hz) indicates that H-1/14 and H-2/15 are in an anti-conformation. Additional experiments are needed to fully elucidate the relative conformation and configuration of these atoms, however the [α]$_D$ values of **1**-**3** ranged from -26 to -27. The optical rotation of **4** could not be measured due to the low yield of the compound. The [α]$_D$ values for **1**-**3** were similar to the value (-20) reported for **11**.[23] In addition, the CD spectrum of **1** was similar to the CD spectrum reported for cylindrocyclophane A.[23] Based on these similarities, we submit that **1**-**4** have the same absolute configuration at C-1/14, C-2/15, and C-7/20 as **11**.

The $^3J_{H-1,H-2}$ values for **5**-**8** showed similar values (9.6-10.4 Hz), which is also consistent with an anti-conformation of H-1 and H-2. The [α]$_D$ values for cylindrocyclophanes C_1-C_4 (-37 to -44) were also similar to the value reported for **12** (-40).[23] Based on these similarities, we submit that **5**-**8** also have the same absolute configuration at C-1/14, C-2/15, and C-7/20 as **12**.

The yield of **9** was not sufficient to determine the [α]$_D$ value for this compound. However, given the stereochemical similarities found for **1**-**8** and **11**-**13**, we submit that **9** should have the same absolute configuration at C-1/14, C-2/15, and C-7/20 as the previously reported **13**, because these compounds likely share a common biosynthesis.

Biosynthetic Incorporation of Bromine

Incorporation of halogens, especially chlorine and bromine, is not uncommon in the secondary metabolism of cyanobacteria.[24-26] However, it is important to note that these molecules are often isolated from marine cyanobacteria whereas, the chlorinated cylindrocyclophanes were isolated from a terrestrial cyanobacterium cultured in a freshwater medium (Z). Z medium, like many freshwater, algal culture media, is composed of various inorganic salts dissolved in deionized H_2O. Often many of these salts will have a chloride counter ion for the desired nutrient, e.g. $FeCl_3$ for Fe^{3+} or $MgCl_2$ for Mg^{2+}. An inspection of

Z medium protocol used by the UIC culture collection[27] did not reveal any major components with a chloride counter ion. It was determined that the main source of chloride was due to the use of HCl to adjust the pH of the medium prior to autoclaving. It is estimated that a typical batch of Z medium, using Tris/HCl, has approximately 10^{-2} M Cl$^-$ as compared to seawater with a Cl$^-$ concentration near 0.6 M.

Previous reports of biological halogenation have shown that many of the halogenases have a low specificity for the halide substrate and the halogen preference is typically driven by the relative concentrations of each anion (Cl$^-$, Br$^-$ and I$^-$).[28, 29] With this information in mind, *Nostoc* sp. (UIC 10022A) was cultured in varying concentrations of KBr (0.8, 8.4 and 84 mM) in Z medium devoid of Cl$^-$. The cultures were grown under the same environmental conditions as the original 2 L cultures, i.e. 20 °C with 16/8 h light/dark cycle. After eight weeks of growth, the resulting biomass was harvested via centrifugation then freeze-dried. The lyophilized biomass for the KBr cultures were extracted with CH_2Cl_2:CH_3OH (1:1). Each extract was subjected to HPLC-UV-MS analysis and the LC-MS data for all three of the extracts revealed the presence of several brominated cylindrocyclophanes. In particular, the extracted ion chromatogram for *m/z* 899 revealed a compound with a retention time of 12.82 min. This ion (*m/z* 899) was selected because it represents the major [M-H]$^-$ ion for tetrabrominated cylindrocyclophane A ($C_{36}H_{52}Br_4O_6$). The mass spectrum acquired at t_R 12.82 min displayed a cluster of ion signals from *m/z* 895.0454 to 903.0418 with intensities that were consistent with a tetrabrominated molecule. The LC-MS data also indicated the presence of dibrominated cylindrocyclophane A ([M-H]$^-$, *m/z* 739.2121) and tribrominated cylindrocyclophane A ([M-H]$^-$, *m/z* 817.1344) at t_R 12.43 min as well as dibrominated ([M-H]$^-$, *m/z* 723.2265) and tribrominated cylindrocyclophane C ([M-H]$^-$, *m/z* 803.1473) at t_R 13.92 min.

All three extracts displayed the presence of brominated cylindrocyclophanes and the extracts were combined to yield 272.0 mg. This combined extract was subjected to C_{18} solid-phase extraction with a MeOH mobile phase to prepare the material for preparative HPLC. The MeOH extract (170.4 mg) was subjected to multiple rounds of semi-preparative reversed-phase (C_{18}) HPLC to yield 0.4 mg of tetrabrominated cylindrocyclophane A, which we have named cylindrocyclophane A_{B4} (**10**).

Cylindrocyclophane A_{B4} (**10**) was obtained as white, amorphous solid. The negative mode HRESI-TOF-MS data for **10** indicated a molecular formula of $C_{36}H_{52}Br_4O_6$ ([M-H]$^-$, *m/z* 895.0461) with an isotopic distribution pattern that was consistent with tetrabromination. The ^{1}H NMR spectrum (Table 3) for **10** displayed signals indicaing that this compound followed the same halogenation pattern as **1**. In particular, the ^{1}H NMR spectrum for **10** displayed a triplet at δ_H 5.80 that correlated with δ_C 48.0 in the HSQC spectrum for **10**. These signals were consistent with a dibromomethyl moiety and, considering that all other NMR signals were similar to those for **1**, it was deduced that **10** is 30,30,34,34-tetrabromocylindrocyclophane A. The proton and carbon chemical shifts were assigned by comparing the NMR data for **1** with the NMR data for **10**. Considering that **10** was isolated from the same organism, and thus produced by the same biosynthetic pathway as **1-4**, we submit that **10** would have the same absolute configuration as **1-4**.

Structure-activity Relationships

Compounds **1-5,7,9-13** were evaluated to determine inhibition of the 20S proteasome. These compounds displayed a wide range of activity with **1-3** being the most potent (IC_{50} = 2.55-3.93 μM) (Table 4). The structurally related **11** and **4** displayed IC_{50} values that were at least seven-fold less potent than **1-3**. A common structural feature of **1-3** is the presence of a dichloromethyl moiety (C-30) at the end of the side chain (C-27 to C-30), while both **11** and

4 lack this moiety on either side chain (C-27/31 to C-30/34). These results indicate that the dichloromethyl moiety of **1**-**3** is important for the biological activity.

A comparison of the biological activity of **11**-**13** revealed that **11** was twice as potent as **12,** while **13** was inactive at a concentration greater than 100 μM. The only structural difference among these molecules is the presence or absence of a hydroxy moiety at C-1 and C-14. The most potent of these three compounds, i.e. **11**, has hydroxy moieties at both C-1 and C-14, while the inactive compound **13** lacks both hydroxy moieties. Based upon these results, we submit that the hydroxy moieties at C-1 and C-14 are important for inhibition of the proteasome. This hypothesis is also supported by the fact that **12**, which has only one hydroxy moiety at C-1, displayed half the potency of **11**. Given that **11** is symmetrical it is possible that both hydroxy moieties (C-1 and C-14) are not required for binding but rather that the C_2 axis of symmetry of the molecule would decrease the entropy of binding.

The initial comparison of the structures and related activities for **4** and **3** revealed the importance of the dichloromethyl moiety (C-30/34) and the comparison of **11**-**13** revealed the importance of the benzylic hydroxy moiety (C-1/14) for the biological activities of these compounds. A comparison of the structures and activities of **3**, **5**, and **7** was used to join these two "pharmacophores". The structure of **7** was important to this study since the dichloromethyl (C-30) and the benzylic hydroxy moiety (C-1) were "distal" (Figure 2, dashed line), while the benzylic carbon (C-14) that was "adjacent" (Figure 2, solid line) lacked a hydroxy group. In the structure of **3**, both benzylic carbons (C-1 and C-14) possessed an attached hydroxy group. Biological evaluation of **7** (IC_{50} = 22.8 ± 2.7 μM) revealed that it was more than eight-fold less potent as proteasome inhibitor than **3** (IC_{50} = 2.55 ± 0.11 μM). Based upon these results, it was apparent that the "adjacent" relationship of the benzylic hydroxy and the dichloromethyl moiety was important for inhibition of the proteasome. The importance of the "adjacent" relationship was also confirmed by the activity of **5** (Figure 2). The difference between the structures of **7** and **5** is that the methyl group (C-34) that is "adjacent" to the benzylic hydroxy moiety (C-1) is dichlorinated in **5**, while C-34 is not modified in **7**. As with the comparison of **3** and **5**, the molecule containing a dichloromethyl moiety "adjacent" to a benzylic hydroxy (**5**), was more potent (IC_{50} = 11.2 ± 1.23 μM) than the molecule that lacked this relationship (**7**, IC_{50} = 22.8 ± 2.7 μM).

The final part of this preliminary SAR investigation was the comparison of **1** and **10**. The difference between these two molecules is the halogen present in the dihalogenated methyl moiety, Cl for **1** and Br for **10**. Both compounds displayed similar potencies (IC_{50} = 3.93 ± 0.18 and 2.23 ± 0.48 μM for **1** and **10**, respectively), indicating that the type of halogen, i.e. Cl or Br, is not as important to the level of activity as the other structural features described previously.

The cytotoxicity EC_{50} values (Table 4) for **1**-**3**, **5**, **7**, and **10** did not reveal any variation that could be used to elucidate any structure-activity relationships. While evaluation of all of the cylindrocyclophanes could produce some variation that could be used for SAR studies, it is important to note that the EC_{50} values acquired during this project (0.9-2.8 μM) were similar to the cytotoxic potencies reported by Moore et al. (0.5-5 μg/mL) for cylindrocyclophanes A-F and Bui et al. (3.3-5.1 μM) for carbamidocyclophanes A-C.[21, 22] Based upon these reports and the data acquired here, we do not anticipate any significant difference in the cytotoxic activity of the chlorinated cylindrocyclophanes as compared to **11**-**13**, thus making any SAR studies difficult. Also, it is important to note that **7**, which displayed proteasome inhibition that was more than seven-fold less potent than **3**, displayed similar cytotoxicity (EC_{50} = 0.9 μM and EC_{50} = 1.7 μM, respectively) as **3**. Based upon these results, it is unlikely that inhibition of the proteasome is the primary mode of action for the cytotoxicity of these compounds.

Taxonomic Identification

The initial taxonomic identification of UIC 10022A was conducted using traditional techniques, i.e. morphological analysis. The morphological features (see Supporting Information) suggested that this strain was a member of the genus *Nostoc*,[30-32] however the genus *Trichormus* could not be definitively ruled out solely on morphological analysis. Therefore, it was important to compare genetic material of UIC 10022A with reference strains of the genera *Nostoc* and *Trichormus*.

The genetic analysis of UIC 10022A was performed using a 1.2 kb sequence of the 16S rRNA gene. For the phylogenetic comparison, reference sequences were first selected using the list of reference strains found in *Bergey's Manual of Systematic Bacteriology*.[33] Only sequences of at least 1 kb were retrieved from GenBank. For the genus *Nostoc*, the reference strains were PCC73102, PCC6720, PCC7120, and PCC7423. Strains for the genus *Trichormus* were also added to allow a phylogenetic comparison of UIC 10022A with that genus.[34] In addition, the cryptophycin producing *Nostoc* strains GSV224 and ATCC53789 and the cylindrocyclophane A-F producing *Cylindrospermum lichenforme* UTEX2014 were also added.

A BLAST search of the UIC 10022A 16S rRNA sequence was employed to retrieve sequence data for the phylogenetic analysis. Top scoring sequences included in the phylogenetic analysis were from the strains *Nostoc* sp. PCC7423, *Nostoc* sp. KK-01, *Nostoc muscorum* CENA61, *Anabaena flos-aquae* UTCC64, and *Anabaena variabilis* ATCC29413. Phylogenetic trees were constructed using neighbor joining (NJ), maximum parsimony (MP), and minimum evolution (ME) methods. In all three cases, the resulting phylogenetic trees had similar topology near the node for UIC 10022A and the *Nostoc* cluster containing UIC 10022A was identical for all trees with the same bootstrap value. The minimum evolution tree (ME) (Figure 3) revealed that the 16S rRNA sequence for UIC 10022A was a member of a monophyletic clade that included the *Nostoc* sp. strains PCC7423, KK-01, and CENA61. According to *Bergey's Manual of Systematic Bacteriology*, PCC7423 is the reference strain for *Nostoc* cluster 3.3, thus we gave that clade the same designation.[33] The phylogenetic tree also revealed that reference strains for the genus *Trichromus* did form a monophyletic clade, but this cluster was quite distant from *Nostoc* cluster 3.3. These results support the taxonomic assignment of *Nostoc* sp. to UIC 10022A.

Quite surprisingly, the phylogenetic tree also revealed that *Nostoc* cluster 3.3 was not part of a strong, monophyletic clade with other "Bergey's" reference *Nostoc* strains, i.e. PCC73102, PCC6720, and PCC7120. In particular, the node for *Nostoc punctiforme* PCC73102, reference strain for *Nostoc* cluster 1,[33] was a member of a monophyetic clade that included the cryptophycin producing strains GSV224 and ATCC29413. However, the clade that included both *Nostoc* clusters 1 and 3.3 also included reference strains from other genera, specifically *Tolypothrix* spp. PCC7504 and PCC7415, *Anabaena* sp. PCC7108, and *Cylindrospermum stagnale* PCC7417. Further study of these organisms, e.g. the phylogenetic analysis of additional genes such as ITS, rpoB, rpoC, and rbcL/rbcX, would be required to determine the taxonomic implications of the heterogeneity found in this clade.

It is also important to note that that both *Cylindrospermum* strains previously reported to produce cylindrocyclophanes formed a monophyletic clade that was not closely associated with the clade that included *Nostoc* sp. UIC 10022A. Considering the evolutionary distance between these organisms and the heterogeneity of the group that includes all three cylindrocyclophane producing cyanobacteria, it is possible that the biosynthetic genes were shared via horizontal gene transfer between the *Cylindrospermum* and *Nostoc* species. Further genetic analysis of members of both genera would be needed to validate this hypothesis.

Experimental Section

General Experimental Procedures

Optical rotations were determined on a Perkin-Elmer 421 polarimeter. UV spectra were obtained on a Varian Cary 50 Bio spectrophotometer. CD spectra were obtained on a Jasco J-710 spectropolarimeter. IR spectra were obtained on a Jasco FTIR-40 Fourier transform infrared spectrometer. The NMR spectra were acquired at 600 MHz for ^{1}H and 226 MHz for ^{13}C on Bruker DRX600 MHz and Bruker AVII900 MHz NMR spectrometers, respectively. The TOF-MS was acquired on a Shimadzu IT-TOF spectrometer. HPLC separations were performed on a Thermo HPLC system consisting of a P4000 pump and UV1000 UV absorbance detector. HPLC-UV-MS analyses were performed on a Shimadzu Prominence liquid chromatograph with UV-Vis photodiode array detector and the above mentioned IT-TOF mass spectrometer.

Biological Material

A *Nostoc* sp. (10022A) was isolated from an algal assemblage growing on the soil in a parkway in the 400 block of West Melrose Avenue in Chicago, Illinois (N 41° 56.46′ W 87° 38.39′). The unialgal strain (10022A) was produced through a combination of streak plate and micropipette isolation techniques.[16] The strain was cultured in 2 L of Z medium[27] in 2.8 L Fernbach flasks and 20 L of Z medium in a 22 L glass carboy, both with sterile aeration. After 6-8 weeks of growth, the cultures were harvested by centrifugation and then freeze dried.

Strain Identification

Cultured material was used for both morphological studies and phylogenetic analysis. Microscopic observation was performed using a Zeiss Axiostar Plus light microscope. The following parameters were utilized for identification: thallus morphology, relative size and shape of vegetative cells, presence and arrangement of heterocytes, presence, relative size of akinetes, trichome polarity, end cell morphology, and colony structure (see Supporting Information). Identification by phenotype was performed according to the system by Komárek *et al*.[30]

DNA Extraction, 16S rDNA PCR Amplification, and Sequencing

Prior to DNA extraction, 8 mL of a static culture of *Nostoc* sp. (UIC 10022A) was combined with 1.5 mL of 100 mM HEPES/NaOH, pH 6.8, 10 mM EDTA and 0.5 mL of 10 mg/mL lysozyme then incubated in a 35 °C water bath for 1 h. After incubation, the cell material was recovered via centrifugation and transferred to a clean 2 mL microcentrifuge tube. DNA was extracted from the resulting cell material using the Wizard Genomic DNA purification kit (Promega). The manufacturer's protocol was modified to include mechanical disruption after the addition of the nuclei lysis solution (step 6). A portion of the 16S rDNA gene was amplified by PCR from the DNA using the cyanobacterial specific primers 106F and 1509R previously described by Nubel et al.[35] Reaction mixtures consisted of 1 μL of DNA (100 ng), 4 μL of 5× Phusion HF buffer, 0.4 μL of dNTP mix (10 μM of dATP, dCTP, dGTP, and dTTP), 1 μL of each primer (10 μM), 0.2 μL of Phusion high-fidelity DNA polymerase (New England Biolabs cat. F-530S), and 12.6 μL of H_2O for a total volume of 25 μL. The reaction was performed using a Bio-Rad C1000 Thermal Cycler with the following reaction program: initial denaturation for 130 s at 98 °C, 24 cycles of amplification with 10 s at 95 °C, 30 s at 50 °C, and 60 s at 72 °C, and a final elongation of 3 min at 72 °C. PCR products were purified using the MinElute PCR purification kit from Qiagen and sequenced in both directions using the previously described cyanobacterial primers (106F and 1509R) as well

as internal primers 359F and 781R.[35] The resulting sequence was deposited with NCBI Genbank (acc. no. HM359085).

Phylogenetic Analysis

Phylogenetic analyses were conducted in MEGA4.[36] The resulting sequence chromatograms were visually inspected and the total sequence of 1215 nucleotides was aligned with 41 cyanobacterial species obtained from GenBank (http://www.ncbi.nlm.nih.gov), as well as the evolutionary distant *E. coli* ATCC8739. Multiple sequence alignment was performed via the ClustalW interface of MEGA4 using default gap opening (15) and extension (6.66) penalties. The aligned sequences were used to construct phylogenetic trees in MEGA4. The evolutionary history was inferred using the neighbor-joining (NJ), minimum evolution (ME), and maximum parsimony (MP) methods. For each method, the bootstrap consensus tree inferred from 1000 replicates was taken to represent the evolutionary history of the taxa analyzed.

Extraction and Dereplication

Two 2 L cultures of 10022A (0.92 g lyophilized biomass) were extracted with 1:1 CH_2Cl_2:CH_3OH to yield 110.9 mg of extract. The extract (83.5 mg) was subjected to flash chromatography utilizing HP20SS Diaion resin and a H_2O:IPA step gradient (1:0, 4:1, 3:2, 2:3, 3:7, 1:4, 1:9, 0:1) to yield eight fractions. A portion (5.0 mg) of fraction 4 (8.50 mg) was subjected to semi-preparative HPLC (Agilent Series 1100, Phenomenex Onyx C_{18}, 4.6 × 100 mm, H_2O:MeCN) to yield 32 fractions collected in a 96 deep well plate. The collected material was dried *in vacuo* and resuspended in MeOH to create daughter plates for biological evaluation and ESI-TOF-MS analysis. The remaining material was again dried in vacuo and select fractions were resuspended in MeOH-d_4 for ^{1}H NMR analysis.

Isolation of Chlorinated Cylindrocyclophanes

A 20 L culture of 10022A (12.76 g lyophilized biomass) yielded 557.8 mg of extract (CH_2Cl_2:CH_3OH 1:1). This extract was subjected to flash chromatography utilizing HP20SS Diaion resin and a H_2O:IPA gradient to yield eight fractions. These fractions were subjected to HPLC-ESI-TOF-MS analysis to determine the presence of cylindrocyclophanes. Multiple rounds of semi-preparative reversed-phase HPLC of F4 (Varian Dynamax C_{18}, 10×250 mm, H_2O:MeOH) yielded 4.7, 0.5, 1.6, 0.3, 0.8, 1.1, 2.0, 0.5, 0.1, 0.3, 0.3, and 0.1 mg of **1-9** and **11-13**, respectively. The elution order of the cylindrocyclophanes was **4**, **11**, **2**, **3**, **1**, **8**, **12**, **6**, **7**, **5**, **13**, and **9**.

Culture in KBr Enriched Media

Three separate 2 L cultures of 10022A were grown in the presence of 0.1, 1.0 and 10.0 g/L KBr, respectively. The base Z medium for each culture was modified by substituting Tris/HCl with Tris/H_2SO_4 to reduce the concentration of chloride. The cultures were grown under the same environmental conditions as the original 2 L cultures. After eight weeks of growth, the resulting biomass was harvested via centrifugation and freeze dried. The lyophilized biomass for the 0.1, 1.0 and 10.0 g/L KBr cultures (1.03, 1.05 and 0.49 g, respectively) was extracted with CH_2Cl_2:CH_3OH (1:1) to yield 95.4, 113.8 and 106.8 mg, respectively. For each extract, 5 μL of a 10 mg/mL MeOH solution was subjected to HPLC-UV-MS analysis (Shimadzu Prominence liquid chromatograph, Varian Microsorb 100-5 C_{18}, 2.0 × 250 mm, 5% MeOH$_{(aq)}$ with 0.1% acetic acid:MeOH). Chromatographic data were acquired for UV-Vis absorbance (photodiode array detector, λ: 200-700 nm) and HRESI-TOF-MS (scan events: (+) *m/z* 100-500, (+) *m/z* 400-2000, (-) *m/z* 100-500, and (-) *m/z* 400-2000).

Isolation of Cylindrocyclophane A$_{B4}$

The extracts of the three KBr cultures were combined to yield 272.0 mg. This combined extract was subjected to C$_{18}$ solid phase extraction with a MeOH mobile phase to prepare the material for preparative HPLC. The MeOH extract (170.4 mg) was subjected to multiple rounds of semi-preparative reversed-phase HPLC (Varian Dynamax C$_{18}$, 10×250 mm, H$_2$O:MeOH) to yield 0.4 mg of **10**.

Cylindrocyclophane A$_4$ (1)—White amorphous powder; [α]$_D$-26 (*c* 0.2, MeOH); UV(MeOH) λ$_{max}$ (log ε) 227 (3.88), 274 (3.17) nm; CD (c 0.006, MeOH) λ$_{max}$ (Δε) 207 (6.4), 218 (-3.2), 247 (-0.13), 261 (0.21), 281 (-1.0) nm; IR (neat) ν$_{max}$ 3266 (br), 2926, 1594, 1431, 1018, 951, 838, 804 cm^{-1}; ^{1}H and ^{13}C NMR see Table 1; HR-ESI-TOF-MS (-) *m/z* 719.2392 [M-H]- (calcd for C$_{36}$H$_{51}$Cl$_4$O$_6$, 719.2445).

Cylindrocyclophane A$_3$ (2)—White amorphous powder; [α]$_D$ -27 (*c* 0.06, MeOH); UV(MeOH) λ$_{max}$ (log ε) 217 (4.04), 279 (3.18) nm; IR (neat) ν$_{max}$ 3283 (br), 2928, 2856, 1594, 1431, 1016, 950, 842 cm^{-1}; ^{1}H and ^{13}C NMR see Table 1; HR-ESI-TOF-MS (-) *m/z* 685.2877 [M-H]$^-$ (calcd for C$_{36}$H$_{52}$Cl$_3$O$_6$, 685.2835).

Cylindrocyclophane A$_2$ (3)—White amorphous powder; [α]$_D$ -26 (*c* 0.07, MeOH); UV(MeOH) λ$_{max}$ (log ε) 227 (3.88), 274 (3.21) nm; IR (neat) ν$_{max}$ 3259 (br), 2927, 2855, 1594, 1431, 1372, 1017, 949, 843 cm^{-1}; ^{1}H and ^{13}C NMR see Table 1; HR-ESI-TOF-MS (-) *m/z* 651.3257 [M-H]$^-$ (calcd for C$_{36}$H$_{53}$Cl$_2$O$_6$, 651.3225).

Cylindrocyclophane A$_1$ (4)—White amorphous powder; UV(MeOH) λ$_{max}$ (log ε) 212 (3.79), 274 (2.62) nm; IR (neat) ν$_{max}$ 3401 (br), 2927, 2855, 1629, 1430, 1375, 1232, 1091, 1016, 986, 828 cm^{-1}; ^{1}H and ^{13}C NMR see Table 1; HR-ESI-TOF-MS (-) *m/z* 617.3639 [M-H]$^-$ (calcd for C$_{36}$H$_{54}$ClO$_6$, 617.3818).

Cylindrocyclophane C$_4$ (5)—White amorphous powder; [α]$_D$ -40 (*c* 0.03, MeOH); UV(MeOH) λ$_{max}$ (log ε) 229 (3.66), 270 (2.53) nm; IR (neat) ν$_{max}$ cm^{-1}; ^{1}H and ^{13}C NMR see Table 2; HR-ESI-TOF-MS (-) *m/z* 703.2469 [M-H]$^-$ (calcd for C$_{36}$H$_{51}$Cl$_4$O$_5$, 703.2496).

Cylindrocyclophane C$_3$ (6)—White amorphous powder; [α]$_D$ -39 (*c* 0.05, MeOH); UV(MeOH) λ$_{max}$ (log ε) 216 (3.74), 274 (2.94) nm; IR (neat) ν$_{max}$ 3310 (br), 2930, 1629, 1429, 1374, 1011 cm^{-1}; ^{1}H and ^{13}C NMR see Table 2; HR-ESI-TOF-MS (-) *m/z* 669.2858 [M-H]$^-$ (calcd for C$_{36}$H$_{52}$Cl$_3$O$_5$, 669.2886).

Cylindrocyclophane C$_2$ (7)—White amorphous powder; [α]$_D$ -37 (*c* 0.15, MeOH); UV(MeOH) λ$_{max}$ (log ε) 227 (3.83), 274 (3.14) nm; IR (neat) ν$_{max}$ 3233 (br), 2925, 2855, 1512, 1429, 1015, 949, 854 cm^{-1}; ^{1}H and ^{13}C NMR see Table 2; HR-ESI-TOF-MS (-) *m/z* 635.3247 [M-H]- (calcd for C$_{36}$H$_{53}$Cl$_2$O$_5$, 635.3276).

Cylindrocyclophane C$_1$ (8)—White amorphous powder; [α]$_D$ -44 (*c* 0.05, MeOH); UV(MeOH) λ$_{max}$ (log ε) 227 (3.33), 274 (2.78) nm; IR (neat) ν$_{max}$ 3319 (br), 2931, 2859, 1631, 1458, 1429, 1374, 1090, 1055, 1010, 831 cm^{-1}; ^{1}H and ^{13}C NMR see Table 2; HR-ESI-TOF-MS (-) *m/z* 601.3643 [M-H]$^-$ (calcd for C$_{36}$H$_{54}$ClO$_5$, 601.3665).

Cylindrocyclophane F$_4$ (9)—White amorphous powder; UV(MeOH) λ$_{max}$ 219, 270 nm; IR (neat) ν$_{max}$ cm^{-1}; ^{1}H and ^{13}C NMR see Table 3; HR-ESI-TOF-MS (-) *m/z* 687.2618 [M-H]$^-$ (calcd for C$_{36}$H$_{51}$Cl$_4$O$_4$, 687.2547).

Cylindrocyclophane A$_{B4}$ (10)—White amorphous powder; $[\alpha]_D$ -45 (*c* 0.04, MeOH); UV(MeOH) λ_{max} (log ε) 227 (3.90), 274 (3.54) nm; IR (neat) ν_{max} 3318 (br), 2923, 2854, 1595, 1430, 1374, 1013, 832 cm^{-1}; ^{1}H and ^{13}C NMR see Table 3; HR-ESI-TOF-MS (-) *m/z* 895.0461 [M-H]$^-$ (calcd for C$_{36}$H$_{51}$Br$_4$O$_4$, 895.0425).

20S Proteasome Bioassay

Evaluation of inhibition of the 20S proteasome was performed as previously described.[16]

HT-29 assay

Cytotoxicity against the HT-29 cancer cell line was performed according to established protocols.[37]

Supplementary Material

Refer to Web version on PubMed Central for supplementary material.

Acknowledgments

References and Notes

1. Welker, M. Cyanobacterial Hepatotoxins: Chemistry, Biosynthesis, and Occurrence. In: Botana, LM., editor. Seafood and Freshwater Toxins. CRC Press; Boca Raton, FL: 2008. p. 825-843.

2. Gademann K, Portmann C. Curr Org Chem. 2008; 12:326–341.

3. Burja AM, Banaigs B, Abou-Mansour E, Burgess JG, Wright PC. Tetrahedron. 2001; 57:9347–9377.

4. König GM, Kehraus S, Seibert SF, Abdel-Lateff A, Mueller D. ChemBioChem. 2006; 7:229–238. [PubMed: 16247831]

5. Tan LT. Phytochemistry. 2007; 68:954–979. [PubMed: 17336349]

6. Schwartz RE, Hirsch CF, Sesin DF, Flor JE, Chartrain M, Fromtling RE, Harris GH, Salvatore MJ, Liesch JM, Yudin K. J Ind Microbiol. 1990; 5:113–123.

7. Wagner MM, Paul DC, Shih C, Jordan MA, Wilson L, Williams DC. Cancer Chemother Pharmacol. 1999; 43:115–125. [PubMed: 9923816]

8. Edelman MJ, Gandara DR, Hausner P, Israel V, Thornton D, DeSanto J, Doyle LA. Lung Cancer. 2003; 39:197–199. [PubMed: 12581573]

9. D'Agostino G, Del Campo J, Mellado B, Izquierdo MA, Minarik T, Cirri L, Marini L, Perez-Gracia JL, Scambia G. Int J Gynecol Cancer. 2006; 16:71–76. [PubMed: 16445613]

10. Golakoti T, Yoshida WY, Chaganty S, Moore RE. J Nat Prod. 2001; 64:54–59. [PubMed: 11170666]

11. Ploutno A, Carmeli S. J Nat Prod. 2000; 63:1524–1526. [PubMed: 11087597]

12. Mehner C, Muller D, Kehraus S, Hautmann S, Gutschow M, Konig GM. ChemBioChem. 2008; 9:2692–2703. [PubMed: 18924217]

13. Okino T, Qi S, Matsuda H, Murakami M, Yamaguchi K. J Nat Prod. 1997; 60:158–161.

14. Ploutno A, Carmeli S. Tetrahedron. 2002; 58:9949–9957.

15. Murakami M, Sun Q, Ishida K, Matsuda H, Okino T, Yamaguchi K. Phytochemistry. 1997; 45:1197–1202.

16. Chlipala G, Mo S, de Blanco EJC, Ito A, Bazarek S, Orjala J. Pharm Biol. 2009; 47:53–60. [PubMed: 21430788]

17. Burger AM, Seth AK. Eur J Cancer. 2004; 40:2217–2229. [PubMed: 15454246]

18. Khan T, Stauffer JK, Williams R, Hixon JA, Salcedo R, Lincoln E, Back TC, Powell D, Lockett S, Arnold AC, Sayers TJ, Wigginton JM. J Immunol. 2006; 176:6302–6312. [PubMed: 16670342]

19. Ciechanover A. Cell. 1994; 79:13–21. [PubMed: 7923371]

20. Adams J. Cancer Cell. 2004; 5:417–421. [PubMed: 15144949]

21. Moore BS, Chen J, Patterson GML, Moore RE. Tetrahedron. 1992; 48:3001–3006.

22. Bui HTN, Jansen R, Pham HTL, Mundt S. J Nat Prod. 2007; 70:499–503. [PubMed: 17311455]

23. Moore BS, Chen J, Patterson GML, Moore RE, Brinen LS, Kato Y, Clardy J. J Am Chem Soc. 1990; 112:4061–4063.

24. Marquez BL, Watts KS, Yokochi A, Roberts MA, Verdier-Pinard P, Jimenez JI, Hamel E, Scheuer PJ, Gerwick WH. J Nat Prod. 2002; 65:866–871. [PubMed: 12088429]

25. Orsini MA, Pannell LK, Erickson KL. J Nat Prod. 2001; 64:572–577. [PubMed: 11374946]

26. Orjala J, Gerwick WH. J Nat Prod. 1996; 59:427–430. [PubMed: 8699186]

27. Falch BS, König GM, Wright AD, Sticher O, Angerhofer CK, Pezzuto JM, Bachmann H. Planta Med. 1995; 61:321–328. [PubMed: 7480178]

28. Eustaquio AS, Pojer F, Noel JP, Moore BS. Nat Chem Biol. 2008; 4:69–74. [PubMed: 18059261]

29. Wagner C, El Omari M, Konig GM. J Nat Prod. 2009; 72:540–553. [PubMed: 19245259]

30. Komárek, J.; Komárková, J.; Kling, H. Filamentous Cyanobacteria. In: Wehr, JD.; Sheath, RG., editors. Freshwater Algae of North America. Academic Press; San Diego: 2003. p. 117-196.

31. Herdman, M.; Castenholz, RW.; Rippka, R. Form-genus VIII Nostoc Vaucher 1803. In: Boone, DR.; Castenholz, RW., editors. Bergey's Manual of Systematic Bacteriology. Vol. 1. Springer; New York: 2001. p. 575-580.

32. Komárek J, Anagnostidis K. Arch Hydrobiol Suppl. 1989; 82:247–345.

33. Castenholz, RW. Phylum BX. Cyanobacteria. In: Boone, DR.; Castenholz, RW., editors. Bergey's Manual of Systematic Bacteriology. Vol. 1. Springer; New York: 2001. p. 473-599.

34. Rajaniemi P, Hrouzek P, Kastovska K, Willame R, Rantala A, Hoffmann L, Komárek J, Sivonen K. Int J Syst Evol Microbiol. 2005; 55:11–26. [PubMed: 15653847]

35. Nubel U, GarciaPichel F, Muyzer G. Appl Environ Microbiol. 1997; 63:3327–3332. [PubMed: 9251225]

36. Tamura K, Dudley J, Nei M, Kumar S. Mol Biol Evol. 2007; 24:1596–1599. [PubMed: 17488738]

37. Seo EK, Kim NC, Mi Q, Chai H, Wall ME, Wani MC, Navarro HA, Burgess JP, Graham JG, Cabieses F, Tan GT, Farnsworth NR, Pezzuto JM, Kinghorn AD. J Nat Prod. 2001; 64:1483–1485. [PubMed: 11720542]
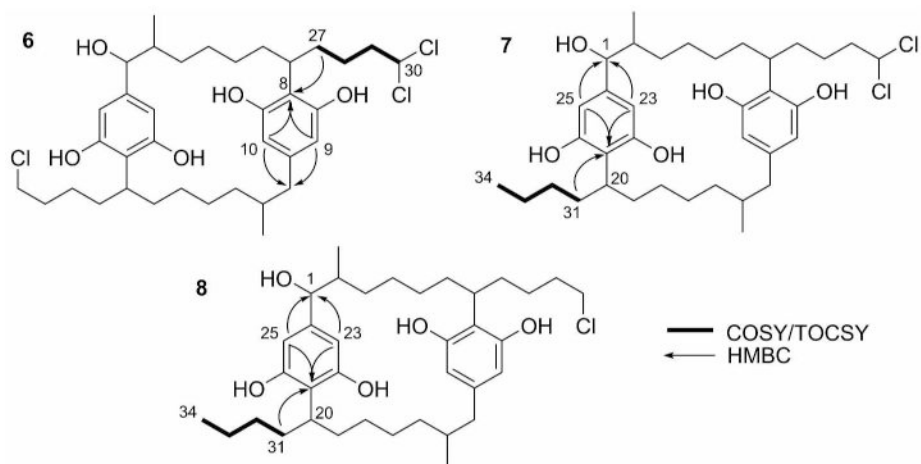
Figure 1.
Key COSY, TOCSY, and HMBC correlations used for assignment of side-chain moieties.
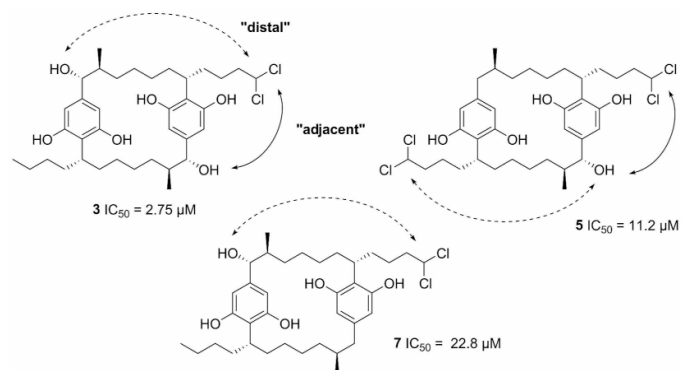
Figure 2.
Chemical structures of **3**, **5**, and **7** with corresponding IC$_{50}$ values for the 20S proteasome bioassay. The key "adjacent" relationship is shown with a solid double arrow.
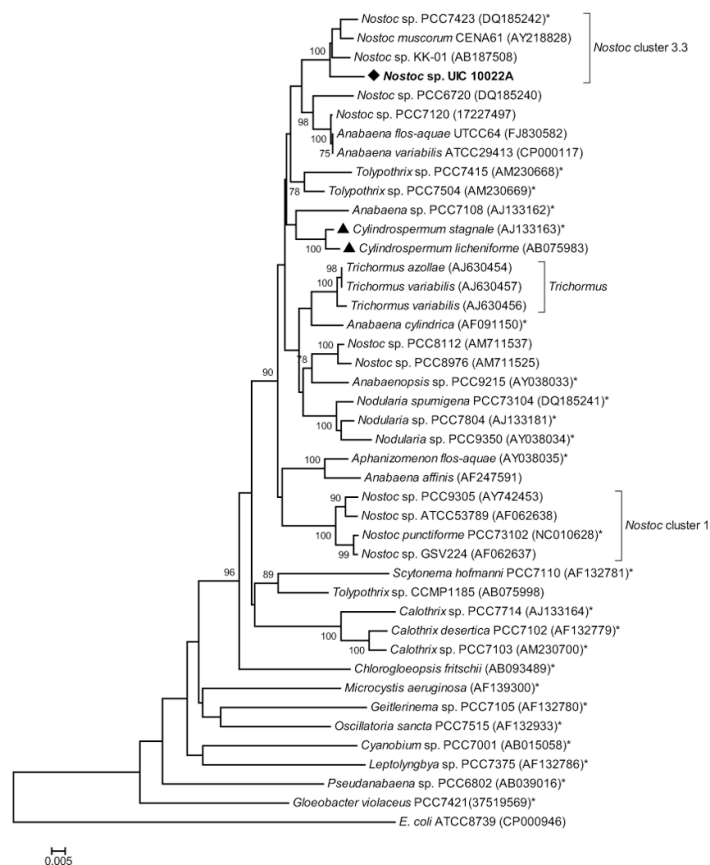
Figure 3.
Phylogenetic relationships of 16S rDNA from cyanobacteria. The tree was constructed using maximum evolution (ME) method with a bootstrap consensus of 1000 replicates. Strains denoted with an asterisk (*) are "Bergey's" reference strains.[33] Cyanobacterial strains previously reported to produce cylindrocyclophanes are denoted by a triangle (▲). Only bootstrap values greater than or equal to 75% are displayed.

Table 1

NMR Data of Cylindrocyclophanes A$_4$-A$_1$ (**1-4**) in MeOH-d_4

| position	cylindrocyclophane A$_4$ (1) δ$_C^a$, mult.	δ$_H^b$ (J in Hz)	cylindrocyclophane A$_3$ (2) δ$_C^c$	δ$_H^b$ (J in Hz)	cylindrocyclophane A$_2$ (3) δ$_C^c$	δ$_H^b$ (J in Hz)	cylindrocyclophane A$_1$ (4) δ$_C^c$	δ$_H^b$ (J in Hz)
1/14	81.8, CH	3.74, d (9.7)	81.6	3.74, d (9.8)	81.5	3.74, d(9.7)	81.8	3.74, d (9.7)
2/15	42.1, CH	1.55, m	41.9	1.55, m	41.9	1.57, m	41.7	1.56, m
3/16a	35.5, CH$_2$	0.73, m	35.0	0.74, m	35.0	0.74, m	35.0	0.75, m
3/16b		0.64, m		0.63, m		0.63, m		0.63, m
4/17a	29.9, CH$_2$	1.42, m	29.7	1.42, m	29.7	1.42, m	29.5	1.42, m
4/17b		0.83, m		0.83, m		0.82, m		0.83, m
5/18a	30.6, CH$_2$	0.95, m	30.3	0.96, m	30.3	0.95, m	30.5	0.95, m
5/18b		0.72, m		0.72, m		0.72, m		0.72, m
6/19a	35.2, CH$_2$	2.07, m	35.2	2.06, m	35.3	2.05, m	35.2	2.05, m
6/19b		1.29, m		1.32, m		1.32, m		1.33, m
7/20	36.4, CH	3.19, m	36.3	3.19, m	36.2	3.19, m	36.5	3.17, m
					36.7	3.15, m	36.6	3.15, m
8/21	116.7, C	-	116.5	-	116.7	-	117.5	-
9/22	159.0, C	-	158.8	-	158.7	-	159.5	-
10/23	105.0, CH	6.25, d (1.2)	104.8	6.25, br s	104.7	6.25, br s	104.8	6.24, br s
11/24	144.2, C	-	143.9	-	143.6	-	144.0	-
12/25	108.8, CH	6.07, d (1.2)	108.6	6.07, br s	108.6	6.07, br s	108.6	6.06, br s
13/26	157.1, C	-	156.9	-	156.6	-	157.5	-
27a	33.8, CH$_2$	2.07, m	33.6	2.06, m	33.6	2.07, m	33.9	2.02, m
27b		1.48, m		1.49, m		1.50, m		1.49, m
28	25.7, CH$_2$	1.35, m	25.4	1.36, m	25.3,	1.35, m	26.3	1.26, m
29a	45.0, CH$_2$	2.20, m	44.8	2.20, m	44.7	2.20, m	33.6	1.76, m
29b		2.06, m		2.06, m		2.06, m		1.65, m
30	75.4, CH	5.82, t (6.2)	75.1	5.82, t (6.1)	75.0	5.82, t (6.1)	45.7	3.43, t (7.4)
31a	33.8, CH$_2$	2.07, m	34.0	2.01, m	34.5	1.94, m	34.4	1.95, m
31b		1.48, m		1.49, m		1.47, m		1.47, m

position	cylindrocyclophane A$_4$ (1)		cylindrocyclophane A$_3$ (2)		cylindrocyclophane A$_2$ (3)		cylindrocyclophane A$_1$ (4)	
	δ$_C$[a], mult.	δ$_H$[b] (J in Hz)	δ$_C$[c]	δ$_H$[b] (J in Hz)	δ$_C$[c]	δ$_H$[b] (J in Hz)	δ$_C$[c]	δ$_H$[b] (J in Hz)
32a	25.7, CH$_2$	1.35, m	26.3	1.25, m	31.4	1.16, m	31.4	1.15, m
32b						1.05, m		1.05, m
33a	45.0, CH$_2$	2.20, m	33.8	1.75, m	23.7	1.25, m	23.8	1.20, m
33b		2.06, m		1.64, m				
34	75.4, CH	5.82, t (6.2)	45.7	3.43, t (6.8)	14.2	0.79, t (7.2)	14.3	0.79, t (7.2)
35/36	17.0, CH$_3$	1.06, d (6.4)	16.6	1.06, d (6.4)	16.7	1.07, d (6.4)	16.7	1.07, d (6.4)

[a]DEPTQ experiment recorded at 226 MHz.

[b]Recorded at 600 MHz.

[c]Determined indirectly using HSQC and HMBC.

Table 2

NMR Data of Cylindrocyclophanes C_4-C_1 (**5-8**) in MeOH-d_4

position	cylindrocyclophane C_4 (**5**) $\delta_C{}^a$	$\delta_H{}^b$ (J in Hz)	cylindrocyclophane C_3 (**6**) $\delta_C{}^a$	$\delta_H{}^b$ (J in Hz)	cylindrocyclophane C_2 (**7**) $\delta_C{}^c$, mutl.	$\delta_H{}^b$ (J in Hz)	cylindrocyclophane C_1 (**8**) $\delta_C{}^a$	$\delta_H{}^b$ (J in Hz)
1	80.9	3.75, d (9.8)	81.7	3.75, d (9.6)	81.8, CH	3.75, d (9.6)	81.4	3.75, d (10.4)
2	41.2	1.57, m	41.2	1.56, m	42.0, CH	1.56, m	41.6	1.57, m
3/16a	35.6	0.75, m	35.2	0.78, m	35.2, CH$_2$	0.75, m	34.8	0.78, m
3/16b		0.64, m		0.65, m		0.62, m		0.65, m
4/17a	29.9	1.44, m	30.0	1.43, m	29.9, CH$_2$	1.41, m	29.7	1.43, m
4/17b		0.83, m		0.81, m		0.81, m		0.81, m
5/18a	30.6	0.96, m	30.3	0.97, m	30.7, CH$_2$	0.96, m	30.4	0.98, m
5/18b		0.75, m		0.74, m		0.74, m		0.74, m
6/19a	34.5	2.06, m	35.3	2.04, m	35.6, CH$_2$	2.06, m	35.1	2.02, m
6/19b		1.34, m		1.33, m		1.30, m		1.32, m
7/20	35.6	3.19, m	36.0	3.16, m	36.3, CH$_2$	3.18, m	36.3	3.15, m
8	114.6	-	115.0	-	115.0, C	-	115.4	-
9	157.9	-	158.2	-	158.4, C	-	158.7	-
10	107.4	6.03, s	107.7	6.03, s	107.9, CH	6.02, s	107.6	6.02, s
11	140.9	-	141.2	-	141.3, C	-	140.7	-
12	110.0	5.98, s	109.7	5.98, s	110.0, CH	5.98, s	109.7	5.97, s
13	156.0	-	157.4	-	157.1, C	-	157.2	-
14a	45.8	2.61, dd (13.2, 3.6)	45.5	2.61, dd (13.2, 3.6)	45.9, CH$_2$	2.61, dd (13.2, 3.6)	45.5	2.61, dd (13.2, 3.6)
14b		1.82, dd (13.2, 11.7)		1.81, dd (13.2, 11.7)		1.83, dd (13.2, 11.7)		1.81, dd (13.2, 11.7)
15	35.7	1.55, m	36.5	1.59, m	36.6, CH	1.58, m	36.5	1.58, m
21	116.4	-	117.3	-	117.8, C	-	117.3	-
22	158.7	-	157.2	-	158.9, C	-	158.7	-
23	104.8	6.25, s	104.8	6.25, s	105.1, CH	6.24, s	104.7	6.24, s
24	143.7	-	144.1	-	143.8, C	-	143.8	-
25	108.5	6.08, s	108.7	6.08, s	108.9, CH	6.07, s	108.5	6.07, s
26	156.6	-	159.1	-	157.0, C	-	157.2	-

position	cylindrocyclophane C$_4$ (5)		cylindrocyclophane C$_3$ (6)		cylindrocyclophane C$_2$ (7)		cylindrocyclophane C$_1$ (8)	
	δ$_C$[a]	δ$_H$[b] (J in Hz)	δ$_C$[a]	δ$_H$[b] (J in Hz)	δ$_C$[c], mutl.	δ$_H$[b] (J in Hz)	δ$_C$[a]	δ$_H$[b] (J in Hz)
27a	35.0	2.06, m	33.9	2.04, m	35.5, CH$_2$	2.05, m	33.8	2.02, m
27b		1.54, m		1.52, m		1.51, m		1.52, m
28	25.2	1.37, m	25.4	1.39, m	25.8, CH$_2$	1.37, m	26.3	1.28, m
29a	44.7	2.20, m	45.0	2.20, m	45.0, CH$_2$	2.20, m	33.6	1.75, m
29b		2.05, m		2.06, m		2.06, m		1.66, m
30	75.1	5.82, t (6.2)	75.2	5.83, t (6.2)	75.4, CH	5.82, t (6.2)	45.5	3.44, t (7.0)
31a	35.0	2.06, m	34.6	2.04, m	34.9, CH$_2$	1.93, m	34.5	1.94, m
31b		1.54, m		1.50, m		1.45, m		1.48, m
32a	25.2	1.37, m	26.8	1.25, m	31.7, CH$_2$	1.18, m	31.5	1.16, m
32b				1.31, m		1.02, m		1.06, m
33a	44.7	2.20, m	33.8	1.75, m	24.0, CH$_2$	1.20, m	23.5	1.29, m
33b		2.05, m		1.65, m				1.21, m
34	75.1	5.82, t (6.2)	45.7	3.43, t (6.9)	14.6, CH$_3$	0.79, t (7.5)	14.2	0.79, t (7.3)
35	16.0	1.06, d (6.4)	16.6	1.06, d (6.4)	16.9, CH$_3$	1.06, d (6.4)	16.7	1.06, d (6.5)
36	20.9	0.95, d (6.5)	20.9	0.95, d (6.5)	20.9, CH$_3$	0.95, d (6.5)	20.5	0.95, d (6.5)

[a]Determined indirectly using HSQC and HMBC.

[b]Recorded at 600 MHz.

[c]DEPTQ experiment recorded at 226 MHz.

Table 3

NMR Data of Cylindrocyclophanes F_4 (**9**) and A_{B4} (**10**) in MeOH-d_4

position	cylindrocyclophane F_4 (**9**)		cylindrocyclophane A_{B4} (**10**)	
	$\delta_C{}^a$	$\delta_H{}^b$ (*J* in Hz)	$\delta_C{}^c$	$\delta_H{}^b$ (*J* in Hz)
1/14a	45.7	2.58, dd (13.6, 3.9)	81.8, CH	3.74, d (9.6)
1/14b		1.83, dd (13.6, 11.0)		
2/15	36.5	1.57, m	42.1, CH	1.55, m
3/16a	36.5	1.02, m	35.2, CH$_2$	0.75, m
3/16b		0.65, m		0.64, m
4/17a	29.8	1.44, m	29.7, CH$_2$	1.43, m
4/17b		0.80, m		0.83, m
5/18a	30.2	0.99, m	30.6, CH$_2$	0.95, m
5/18b		0.78, m		0.73, m
6/19a	35.3	2.01, m	35.2, CH$_2$	2.07, m
6/19b		1.32, m		1.33, m
7/20	36.0	3.16, m	36.4, CH	3.20, m
8/21	114.2	-	116.7, C	-
9/22	n.d.^{d}	-	159.0, C	-
10/23	107.7	6.02, s	105.0, CH	6.25, s
11/24	141.4	-	144.2, C	-
12/25	109.7	5.99, s	108.8, CH	6.07, s
13/26	n.d.^{d}	-	157.1, C	-
27/31a	33.5	2.06, m	33.5, CH$_2$	2.07, m
27/31b		1.50, m		1.51, m
28/32	25.6	1.37, m	27.8, CH$_2$	1.36, m
29/33a	44.8	2.21, m	46.9, CH$_2$	2.41, m
29/33b		2.06, m		2.26, m
30/34	75.1	5.83, t (6.2)	48.0, CH	5.80, t (6.8)
35/36	20.6	0.94, d (6.6)	17.0, CH$_3$	1.07, d (6.4)

[a] Determined indirectly using HSQC and HMBC.

[b] Recorded at 600 MHz.

[c] DEPTQ experiment recorded at 226 MHz.

[d] These atoms could not be assigned due to insufficient signal to noise in the HMBC data.

Table 4

Biological Activity of Isolated Cylindrocyclophanes (**1-5,7,9-13**).

Compound	R_1	R_2	R_3	R_4	20S Proteasome IC_{50} (μM)[a]	HT-29 EC_{50} (μM)[b,c]
1	OH	CHCl$_2$	OH	CHCl$_2$	3.93 ± 0.18	2.0
2	OH	CH$_2$Cl	OH	CHCl$_2$	2.75 ± 0.31	0.5
3	OH	CH$_3$	OH	CHCl$_2$	2.55 ± 0.11	1.7
4	OH	CH$_3$	OH	CH$_2$Cl	27.6 ± 0.6	-
5	OH	CHCl$_2$	H	CHCl$_2$	11.2 ± 1.2	2.8
7	OH	CH$_3$	H	CHCl$_2$	22.8 ± 2.7	0.9
9	H	CHCl$_2$	H	CHCl$_2$	44.8 ± 2.0	-
10	OH	CHBr$_2$	OH	CHBr$_2$	2.23 ± 0.48	0.5
11	OH	CH$_3$	OH	CH$_3$	33.9 ± 3.0	-
12	OH	CH$_3$	H	CH$_3$	59.3 ± 8.2	-
13	H	CH$_3$	H	CH$_3$	> 100	-

Positive controls:

[a] bortezomib (IC_{50} 2.5 nM) and

[b] camptothecin (EC_{50} 60 nM).

[c] A dash (–) denotes the compound was not evaluated.